Journal of Alloys and Compounds 488 (2009) 574–577

Contents lists available at ScienceDirect

Journal of Alloys and Compounds

journal homepage: www.elsevier.com/locate/jallcom

Optical studies of sub-3 nm Eu_2O_3 and Gd_2O_3:Eu^{3+} nanocrystals

Sameer V. Mahajan [a,c], James H. Dickerson [b,c,*]

[a] Interdisciplinary Program in Materials Science, Vanderbilt University, Nashville, TN 37235, United States
[b] Department of Physics and Astronomy, Vanderbilt University, Nashville, TN 37235, United States
[c] Vanderbilt Institute of Nanoscale Science and Engineering, Vanderbilt University, Nashville, TN 37235, United States

ARTICLE INFO

Article history:
Received 3 June 2008
Received in revised form
27 September 2008
Accepted 18 December 2008
Available online 30 December 2008

Keywords:
Nanostructured materials
Rare earth alloys compounds
Phosphors
Optical spectroscopy
Luminescence

ABSTRACT

Colloidally stable sub-3 nm Eu_2O_3 and Gd_2O_3:Eu^{3+} nanocrystals have been synthesized via a hot solution phase technique. Optical properties of the nanocrystals are studied as a function of size. Both nanocrystal compositions exhibit a new optical signature, an emission peak at 620 nm. Intensity modulation of this peak has been observed for all nanocrystal sizes, suggesting surface-dependent or crystal-field dependent effect. Photoluminescence intensity of smaller Eu_2O_3 nanocrystals was comparable to that of the Gd_2O_3:Eu^{3+} nanocrystals.

1. Introduction

Recent progress in the development of rare earth (RE) nanocrystalline materials has focused on new techniques to synthesize these materials to optimize their robust optical and magnetic characteristics [1–11]. Many of their physical traits, such as their small feature size and millisecond luminescence lifetimes, have facilitated the excitement over these materials, making them attractive candidates for a variety of applications, such as high resolution video displays and luminescent probes in bio-imaging applications [12,13]. Thus, the synthesis of monodisperse, colloidally stable, rare earth based nanocrystals and their optical properties are perforce sought for their implementation in bio-imaging applications and for the fabrication of nanocrystalline thin film devices [14,15]. For such biological applications, nanocrystals typically are suspended in fluid environments for which colloidal stability is of prime importance. Colloidal stability suppresses nanocrystal agglomeration and facilitates the manipulation of the surface of individual nanocrystals for bio-conjugation.

Rare earth sesquioxide nanocrystals, such as europium sesquioxide (Eu_2O_3) and RE-doped gadolinium or yttrium sesquioxide (Gd_2O_3:RE^{3+}, Y_2O_3:RE^{3+}; RE = Eu, Tb, Er), have been synthesized in a size-range of 5–100 nm through a number of methods, including gas-phase condensation [1], sol-lyophilization [4], flame pyrolysis [9] and colloidal synthesis [2,3,5,6,10]. The optical properties of RE^{3+} ion based materials originate from 4f–4f electron transitions within RE^{3+} ions [11]. Electrons are excited into the charge-transfer state of the Eu-O bond of sesquioxides (Eu_2O_3 and Gd_2O_3:Eu^{3+}) when excited with ultraviolet radiation ($\lambda = 254$ nm from a xenon lamp, for this study), and subsequently radiative decay of these electrons from ^5D energy levels into ^7F energy levels provide luminescence. Since the core electronic energy levels within Eu^{3+} ions do not change for different particle sizes, the electron transition energies are relatively unaffected by the size of nanocrystals.

The characteristic emission peak, corresponding to $^5D_0 \rightarrow {}^7F_2$ electron transition in Eu^{3+} ions, resides near 612 nm (red) in body-centered-cubic sesquioxides. The energy levels of Eu^{3+} ions change when the ions experience different crystal field environments. The crystal field may change when the atomic arrangement varies from its equilibrium position. Considering the very large surface-to-volume ratio for very small nanocrystals, these materials may experience some lattice distortion, which would lead to a variation in the crystal field. Thus, the optical signature of the nanocrystal may depend on the size of the nanocrystal. To date, there is no report of a study of the optical properties of nanocrystals when their size approaches that of a single lattice constant ($a_0 = 10.86$ Å for Eu_2O_3 and $a_0 = 10.81$ Å for Gd_2O_3).

Here, we report synthesis and optical properties of sub-3 nm Eu_2O_3 and Gd_2O_3:Eu^{3+} nanocrystals as a function of size. The nanocrystal size is controlled via addition of oleic acid (OA)

* Corresponding author at: Department of Physics and Astronomy, Vanderbilt University, Nashville, TN 37235, United States.
E-mail address: james.h.dickerson@vanderbilt.edu (J.H. Dickerson).

0925-8388/$ – see front matter © 2009 Elsevier B.V. All rights reserved.
doi:10.1016/j.jallcom.2008.12.092

Table 1
Comparison of synthesis reaction mixture and nanocrystal size.

RE precursor (mM)	Oleic acid (mM)	Tri-*n*-octylamine (mM)	Nanocrystal size (nm)
0.50	0.00	16.0	~1.8
0.50	0.25	16.0	~2.4
0.50	1.00	16.0	~3.0

during the synthesis. Photoluminescence (PL) measurements of the sub-3 nm Eu_2O_3 and Gd_2O_3:RE^{3+} nanocrystals reveal a new luminescence peak near 620 nm that is not observed in larger nanocrystals or in the bulk. For different nanocrystal sizes, we observed intensity modulations of a new emission peak at 620 nm. Also, photoluminescence intensity of Eu_2O_3 nanocrystals is comparable to Gd_2O_3:Eu^{3+} nanocrystals for smaller nanocrystals sizes.

2. Experimental

Europium(III) chloride hexahydrate ($EuCl_3{\cdot}6H_2O$, 99.99%), gadolinium(III) chloride hexahydrate ($GdCl_3{\cdot}6H_2O$, 99.99%), tri-*n*-octylamine (90.0%), sodium oleate (95%), and oleic acid (90%) were employed for nanocrystal synthesis. The nanocrystals were prepared in a two-stage synthesis as described earlier [8]. First, europium oleate was prepared by heating a mixture of europium chloride hexahydrate and sodium oleate at 60 °C in a water–ethanol–hexane mixture for 4 h. Second, a mixture of europium oleate, oleic acid, and tri-*n*-octylamine (refer to Table 1) was heated to ~350 °C at the rate of 5 °C min^{-1} in an Ar environment and was refluxed for 1 h.

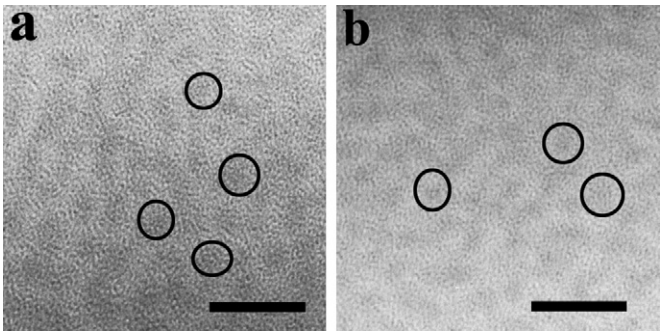

Fig. 1. Nanocrystals of Eu_2O_3 (a) and Gd_2O_3:Eu^{3+} (b) of ~2.4 nm diameter. Scale bar: 12 nm.

During this period, the nucleation and growth of the Eu_2O_3 nanocrystals occurred. For the synthesis of Gd_2O_3:Eu^{3+} (10%) nanocrystals, 0.45 mM gadolinium oleate and 0.05 mM europium oleate were employed, while keeping all other synthesis parameters the same. The size of the nanocrystals was tuned by addition of different amount of oleic acid. The amount of precursors used in the reaction mixture and corresponding nanocrystal size is reported in Table 1. X-ray diffraction measurements were conducted using a Scintag X1 system with a Cu K_α X-ray source. Nanocrystal imaging was performed on a Philips CM 20 transmission electron microscope (TEM) operating at 200 kV. Photoluminescence measurements were performed on nanocrystal dispersions in hexane using a Fluorolog-3 spectrophoto-fluorometer, equipped with a 450 W xenon lamp set at its 254 nm line.

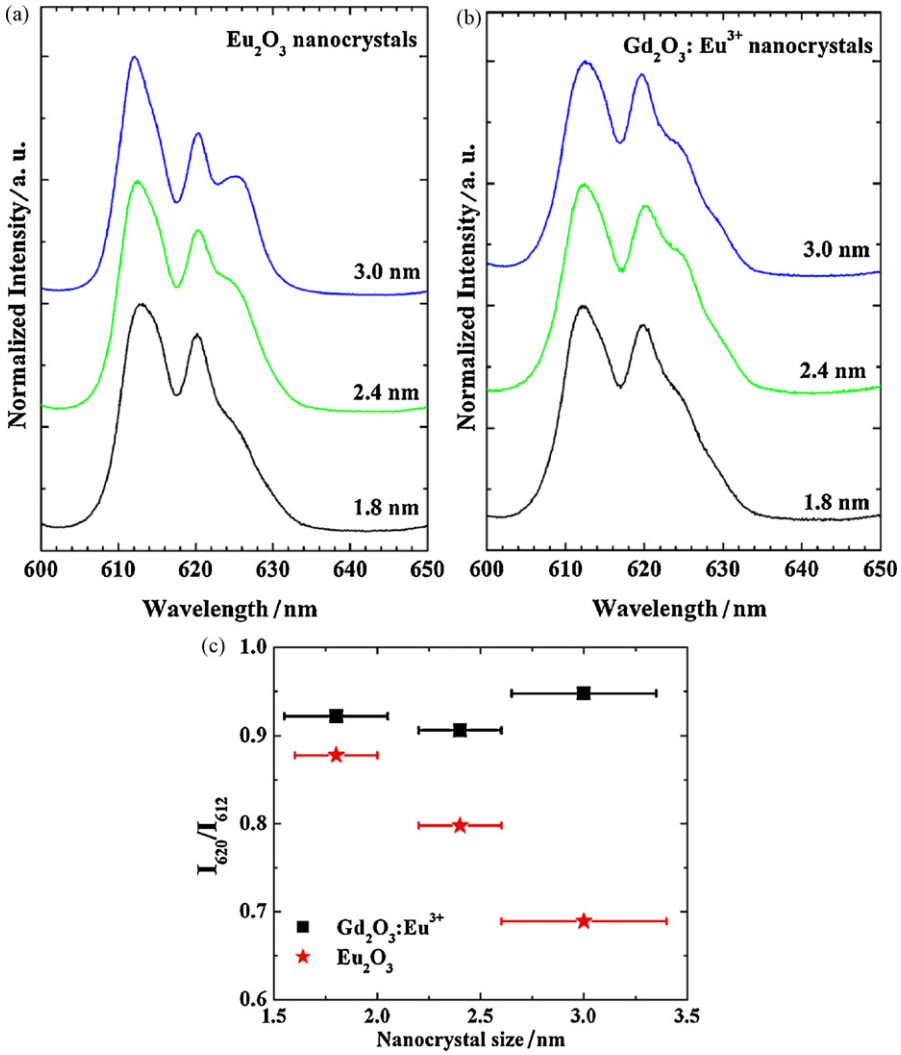

Fig. 2. PL spectra of Eu_2O_3 (a) and Gd_2O_3:Eu^{3+} (b) nanocrystals synthesized with varying amount of OA. The spectra are normalized to the peak at 612 nm and shifted vertically for clarity. (c) The intensity variation of the new peak (620 nm) with respect to the 612 nm peak determined from the above PL spectra.

3. Results and discussion

Synthesis of monodisperse, small size nanocrystals rely on controlled nucleation and growth of oxide nuclei via appropriate precursor and synthesis temperature selection. The pathway for any hot solution phase metal oxide nanocrystal synthesis involving oleic acid includes formation of metal-oleate as a transition stage [16,17]. Therefore, it is advantageous to use Eu/Gd-oleate as Eu^{3+}/Gd^{3+}-precursor for controlled nucleation. In addition, the synthesis temperature (~350 °C) slightly below the decomposition temperature of Eu/Gd-oleate (~370 °C) facilitates slow nucleation and growth of Eu_2O_3/Gd_2O_3 nanocrystals leading to very small size nanocrystals. The size of nanocrystals can also be controlled with addition of oleic acid. The addition of oleic acid facilitated partial redissolution of oxide nuclei and thus, conserving RE-oleate for the nanocrystals growth. Thus, within a small size regime, increased amount of oleic acid produced larger nanocrystals. Amount of oleic acid used in the reaction mixture and corresponding nanocrystal size is reported in Table 1. Fig. 1 shows Eu_2O_3 and Gd_2O_3:Eu^{3+} nanocrystals of 2.4 nm diameter in size.

The optical properties of the Eu^{3+}-based materials derive from 4f–4f electron transitions within the Eu^{3+} ions. Upon excitation of these materials with UV light, the excited electrons decay radiatively from $^5D_0 \rightarrow {}^7F_J$ (J = 0, 1, 2, 3, and 4) energy levels. The characteristic red emission for Eu^{3+}-based materials originates from the $^5D_0 \rightarrow {}^7F_2$ electric dipole transition, which is the most sensitive of the ^7F_J transitions to the position and local environment of Eu^{3+} ions within the crystal lattice. Thus, any changes in the local crystal field surrounding the Eu^{3+} ions will directly result in modification of the peaks arising from $^5D_0 \rightarrow {}^7F_2$ transition.

In Fig. 2a and b, we plot the size-dependent photoluminescence spectra for the Eu_2O_3 and Gd_2O_3:Eu^{3+} nanocrystals. Of substantial interest to us was the emergence of a new luminescence peak at 620 nm, a characteristic which has not been reported in other Eu^{3+}-based rare earth sesquioxide nanostructures. The photoluminescence spectra were recorded for the Eu_2O_3 and Gd_2O_3:Eu^{3+} nanocrystals of different sizes. We attribute the peaks at 612 nm, 620 nm, and 625 nm to the $^5D_0 \rightarrow {}^7F_2$ transition of Eu_2O_3 and Gd_2O_3:Eu^{3+} nanocrystals. The observed peak broadening for our nanocrystals is consistent with that observed for the other nanocrystalline Eu_2O_3 and Gd_2O_3:Eu^{3+} materials [2,4,5,8,18,19]. Comparing the spectra of our nanocrystals with the spectra reported for nanocrystalline and bulk Eu_2O_3 materials, we easily identify the conventional peak for cubic Eu_2O_3 at 612 nm. The peak at 625 nm has been reported for cubic Eu_2O_3 nanodisks, which the authors explained as due to the occupation of Eu^{3+} ions in a unique site due to ultrathin thickness (1.6 nm) of nanodisks [20]. The presence of this spectral feature suggests a similar size-dependent effect on the ^7F_J states in our nanocrystals.

In addition to these luminescence characteristics, we observe a peak at 620 nm, which is a new luminescence peak observed for Eu_2O_3 and Gd_2O_3:Eu^{3+} nanomaterials. In observing this peak for the various nanocrystal sizes, we noticed a variation in the intensity of the peak (620 nm) juxtaposed with the stronger primary peak (612 nm). We monitored the intensity for both nanocrystal types as a function of the nanocrystal size. To simplify the comparison, all the spectra were normalized to the peak at 612 nm. The ratio of intensities of the two peaks ($R = I_{620\,nm}/I_{612\,nm}$) is plotted as a function of nanocrystal size in Fig. 2c. For Eu_2O_3 nanocrystals, the ratio R decreases from 0.88 to 0.70 as nanocrystal size increases. The intensity variation of the peak as a function of nanocrystal size is expected in Gd_2O_3:Eu^{3+} nanocrystals. However, the trend is different to that for the Eu_2O_3 nanocrystals. Intensity modulation of the peak with nanocrystal size could likely be due to occupation of Eu^{3+} ion in a unique surface site, or exposure to an anisotropic crystal field induced because of strain on the surface of very small nanocrystals.

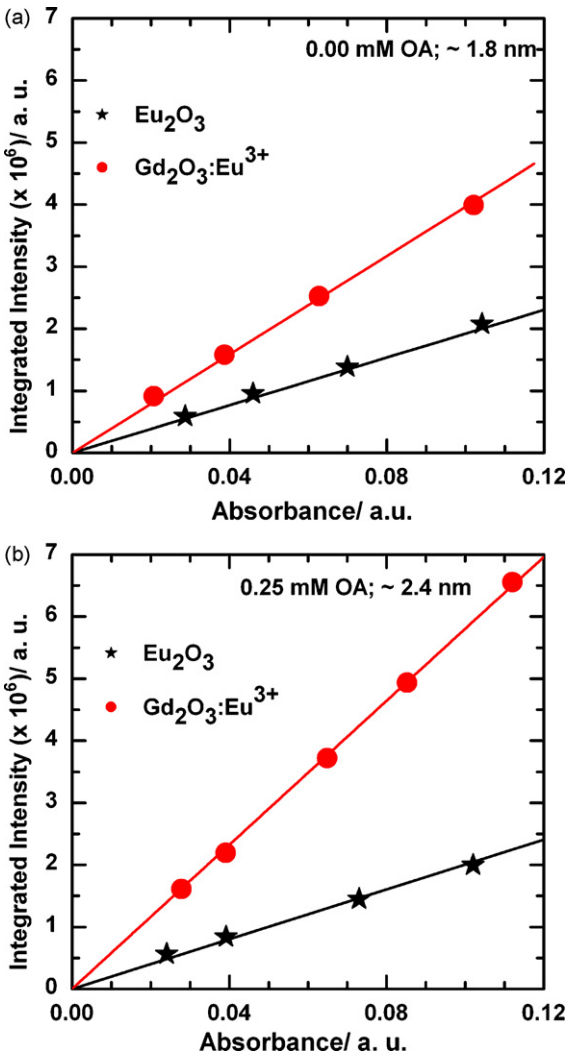

Fig. 3. (a) Integrated PL intensity of (a) ~1.8 nm (no OA) and (b) ~2.4 nm (0.25 mM OA) Eu_2O_3 and Gd_2O_3:Eu^{3+} nanocrystals. The X and Y error bars for the data are within the data point. The solid lines represent liner fit to each dataset.

To continue exploring the effect of nanocrystal size on the photoluminescence intensity of rare earth sesquioxide nanocrystals, we investigated the relationship between the integrated PL intensity and the absorbance of the Eu_2O_3 and Gd_2O_3:Eu^{3+} nanocrystals. The integrated PL intensity of nanocrystals was determined by integrating PL spectra over 525–725 nm wavelength range and is plotted as a function of nanocrystal absorbance, which is shown in Fig. 3a and b for ~1.8 nm and ~2.4 nm Eu_2O_3 and Gd_2O_3:Eu^{3+} nanocrystals. Low absorbance values (or low nanocrystal concentration) are considered to avoid self-quenching effects of nanocrystal suspension. For a given absorbance, 1.8 nm and 2.4 nm Eu_2O_3 nanocrystals have same integrated luminescence intensity. However, the integrated luminescence intensity is lower for 1.8 nm Gd_2O_3:Eu^{3+} nanocrystals than that of 2.4 nm Gd_2O_3:Eu^{3+} nanocrystals. This suggests that luminescence intensities of Eu_2O_3 and Gd_2O_3:Eu^{3+} nanocrystals are comparable for smaller nanocrystal sizes.

4. Conclusion

Sub-3 nm Eu_2O_3 and Gd_2O_3:Eu^{3+} nanocrystals were synthesized by varying the amount of oleic acid during the synthesis. Photolu-

minescence measurements reveal a new optical signature for these nanocrystals, a new luminescence peak at 620 nm. Intensity modulation of the new peak was observed for different nanocrystal size, which could be due to an anisotropic crystal field environment within the nanocrystal or to the occupation of Eu^{3+} ions in unique lattice sites. As the size of the Eu_2O_3 nanocrystals decreased, their associated photoluminescence intensity became comparable to that of the Gd_2O_3:Eu^{3+} nanocrystals.

Acknowledgment

This research is supported in part by Vanderbilt Institute for Nanoscale Science and Engineering (VINSE).

References

[1] H. Eilers, B.M. Tissue, Mater. Lett. 24 (1995) 261–265.
[2] G. Wakefield, H.A. Keron, P.J. Dobson, J.L. Hutchison, J. Colloid Interface Sci. 215 (1999) 179–182.
[3] G. Wakefield, H.A. Keron, P.J. Dobson, J.L. Hutchison, J. Phys. Chem. Solids 60 (1999) 503–508.
[4] C. Louis, R. Bazzi, M.A. Flores, W. Zheng, K. Lebbou, O. Tillement, B. Mercier, C. Dujardin, P. Perriat, J. Solid State Chem. 173 (2003) 335–341.
[5] R. Bazzi, M.A. Flores, C. Louis, K. Lebbou, W. Zhang, C. Dujardin, S. Roux, B. Mercier, G. Ledoux, E. Bernstein, J. Colloid Interface Sci. 273 (2004) 191–197.
[6] R. Bazzi, M.A. Flores-Gonzalez, C. Louis, K. Lebbou, C. Dujardin, A. Brenier, W. Zhang, O. Tillement, E. Bernstein, P. Perriat, J. Lumin. 102 (2003) 445–450.
[7] Y.C. Cao, J. Am. Chem. Soc. 126 (2004) 7456–7457.
[8] S.V. Mahajan, J.H. Dickerson, Nanotechnology 18 (2007) 325605.
[9] D. Dosev, B. Guo, I.M. Kennedy, J. Aerosol Sci. 37 (2006) 402–412.
[10] F. Soderlind, H. Pedersen, J.R.M. Petoral, P.-O. Kall, K. Uvdal, J. Colloid Interface Sci. 288 (2005) 140–148.
[11] S. Shionoya, W.M. Yen, Phosphor Handbook, CRC Press, Boca Raton, 1999.
[12] J. Feng, G. Shan, A. Maquieira, M.E. Koivunen, B. Guo, B.D. Hammock, I.M. Kennedy, Anal. Chem. 75 (2003) 5282–5286.
[13] M. Nichkova, D. Dosev, S.J. Gee, B.D. Hammock, I.M. Kennedy, Anal. Chem. 77 (2005) 6864–6873.
[14] M.A. Islam, Y.Q. Xia, D.A. Telesca, M.L. Steigerwald, I.P. Herman, Chem. Mater. 16 (2004) 49–54.
[15] S.V. Mahajan, D.W. Kavich, M.L. Redigolo, J.H. Dickerson, J. Mater. Sci. 41 (2006) 8160–8165.
[16] J. Park, K.J. An, Y.S. Hwang, J.G. Park, H.J. Noh, J.Y. Kim, J.H. Park, N.M. Hwang, T. Hyeon, Nat. Mater. 3 (2004) 891–895.
[17] T. Hyeon, S.S. Lee, J. Park, Y. Chung, H.B. Na, J. Am. Chem. Soc. 123 (2001) 12798–12801.
[18] B. Bihari, H. Eilers, B.M. Tissue, J. Lumin. 75 (1997) 1–10.
[19] H.S. Yang, H. Lee, P.H. Holloway, Nanotechnology 16 (2005) 2794–2798.
[20] R. Si, Y.W. Zhang, H.P. Zhou, L.D. Sun, C.H. Yan, Chem. Mater. 19 (2007) 18–27.